

Enhanced Nonlinear Pulse Compression from Supercontinuum Generation within Sign-Alternating Dispersion Waveguides

HAIDER ZIA^{1,*}

¹*University of Twente, Department Science & Technology, Laser Physics and Nonlinear Optics Group, MESA+ Research Institute for Nanotechnology, Enschede 7500 AE, The Netherlands*

**h.zia@utwente.nl*

Abstract: Supercontinuum generation (SCG) coherently generates a wide spectrum from a narrow bandwidth optical pulse. We have recently demonstrated a large increase in the bandwidth to input peak power efficiency of the SCG process, by repeatedly alternating the sign of dispersion along a waveguide. Here, novel properties of SCG in these waveguides are explored. Such as their applicability in SCG resonators and a near parabolic SCG spectral phase independent of higher order dispersion along the alternating waveguide. In order to explain this phase independence a previously unknown normal dispersion SCG phase effect is described. The resultant low higher order spectral phase coefficients, combined with the enhanced bandwidth at low input peak powers, than makes alternating dispersion waveguides a scheme that demonstrates potential to extend sub-cycle pulse compression to low input peak powers, removing the need for high powered drive lasers. In addition, a new scheme is shown for the design of practical waveguide segments that can compress SCG pulses to near transform limited durations which is integral for the design of these alternated waveguides. These results are also applicable to general SCG waveguides and nonlinear pulse compression experiments.

1. Introduction

Supercontinuum generation (SCG) in Kerr nonlinear waveguides has been exploited in numerous applications such as in the generation of sub-cycle pulses[1-6], metrology using optical frequency combs[7-11], optical coherence tomography[12-14] and as a wide-bandwidth source for ranging and sensing applications[15,16]. However, spectral generation along the propagation of the waveguides ceases due to the interaction of self-phase modulation (SPM) and dispersion, ultimately limiting the achieved broadened bandwidth [1,2]. We have recently introduced the concept of repeatedly sign-alternating dispersion along the propagation direction as a means of overcoming spectral stagnation that results from this interplay in SCG waveguides (Fig. 1a) [17]. The alternated waveguide structure leads to larger, by potentially several orders of magnitude, input power-to-spectral e^{-1} bandwidth scaling for supercontinuum generation and a flat topped spectral energy density distribution. This is shown in the comparison of our concept with a typical SCG waveguide experiment found in literature [18] (Fig. 1b, 1c).

Here, we consider repeatedly sign-alternating structures where spectral generation occurs primarily in normal dispersion (ND) segments. When spectral generation stagnates due to temporal broadening of the optical pulse, the subsequent anomalous dispersion (AD) segment compresses the pulse to, ideally, its transform limited duration. The temporally compressed pulse then can resume spectral generation in the next ND segment. Limiting SCG to the normal dispersion segments of the alternating waveguide ensures that the SCG has a smooth spectral energy density and phase profile free of modulations.

While our concept opens the possibility to greatly enhance bandwidth generation, many open questions are still unresolved. Firstly, due to the nonlinear generation, the ND and AD segment lengths typically follow a complex arrangement and change along the waveguide. This is inconvenient when periodic arrangements of segment lengths are warranted such as in resonator configurations. Here we report a regime of input pulse parameters where our repeated sign-alternating waveguide has constant ND and AD lengths, independent of input pulse peak power.

Another open question is that the repeated spectral generation and temporal compression of our concept may render that it is sensitive to higher than second order dispersion, practically always present, in the ND and AD segments. For example, this higher order dispersion in the ND and AD segments may introduce a complex spectral phase profile, that impacts temporal compression in the AD segments, limiting the total bandwidth generation. As well, the complex spectral phase that may iteratively build up across the structure would render the concept unfeasible for nonlinear pulse compression experiments. Thus, a solution to this problem would both provide a deeper understanding of what the AD segment GVD profiles need to be and would make our concept feasible as a method for nonlinear pulse compression.

To address this problem, we experimentally found [17] that the maximal amount of higher than second order spectral phase contribution (i.e., at the end points of the spectral bandwidth) is *reduced by more than a factor of three* relative to just linear propagation through the waveguide structure. In this paper, we explain this observation by introducing a previously unknown spectral phase effect of normal dispersion SCG. This effect reduces higher order spectral phase coefficients so that the spectral phase remains near parabolic despite significant uncompensated third order dispersion (TOD). This optical SCG effect is somewhat the compliment to the normal dispersion optical wave-breaking effect [19]. Instead, here, the contributions to higher order spectral phase coefficients of higher order dispersion is in turn reduced by SPM. We find that this robustness to higher order dispersion of the bandwidth generating ND segments, is amplified within our alternating waveguides structures. This effect explains more rigorously why, in general, ND SCG has a near parabolic spectral profile, numerically or experimentally found in various experiments in the last decade [20-23].

Within the context of repeated sign-alternating dispersion SCG waveguides this robustness effect combines a near parabolic spectral phase with a large bandwidth for the output SCG pulse. Thus, these waveguides are a lucrative concept in obtaining large nonlinear pulse compression to sub-cycle durations — at low pump powers. As well, the AD segment GVD profiles that maximize pulse compression can be found from this effect. The concept then opens up the possibility of high-quality nonlinear compression for a greater plethora of optical systems such as for high repetition rate lasers and for the integrated photonics setting.

Practically obtaining the needed AD segment GVD profile then becomes the final open question we address in this paper. The AD segment GVD profiles must satisfy strict requirements on its shape if it were to accomplish maximal pulse compression. Moreover, the AD segment GVD profiles change along the repeated sign-alternating structure, since the bandwidth increases of the ND segments decrease along the structure. To address this open ended question, here, we propose a novel scheme to construct arbitrary AD dispersion profiles by breaking up the AD segment into sub-segments that solve a set of linearly independent equations. This procedure can be used for general pulse compression experiments as well.

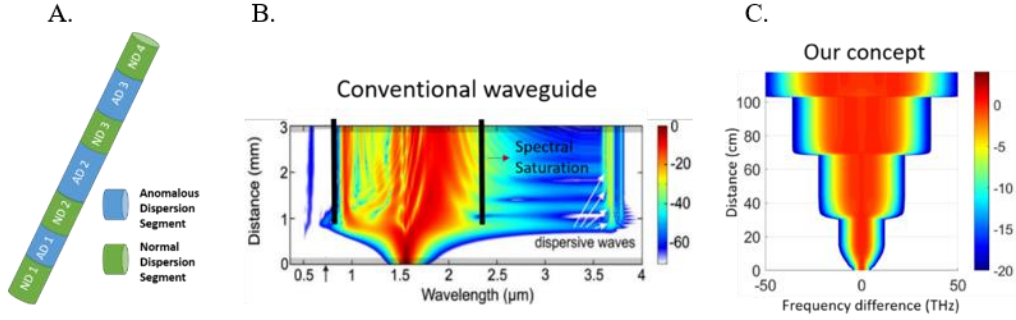


Fig. 1. A) Example schematic of the repeated sign-alternating dispersion waveguide consisting of normal dispersion segments (ND) followed by anomalous dispersion segments (AD). B) Conventional waveguide SCG [18]. Black lines were inserted to highlight the spectral saturation that takes place specifically at the e^{-1} bandwidth (although saturation is visible throughout the entire bandwidth range), past roughly 1 mm of propagation in this particular waveguide. Non-smooth spectral features such as modulations and gaps are clearly visible. C) Plotted is the spectral energy density, in this case, in the spectral generating ND segments of a repeated alternating dispersion waveguide where the AD segments only temporally compress the pulse. The bandwidth increases notably at the e^{-1} level do not saturate versus propagation and the spectrum is smooth and continuous.

2. Periodic Segment Length Convergence

We start by addressing the question of finding ND and AD segment lengths that converge to a fixed arrangement. These segment lengths are set by the amount of spectral broadening that occurs in a segment, and the length until where this spectral broadening saturates, defined as L_{sat} . In general, segment lengths must be chosen for maximum nonlinear generation and best pulse compression for substantial spectral broadening advantages in such structures. Segment lengths are then heavily influenced by the nonlinear length, $L_{nl} = \frac{1}{\gamma P}$, γ being the waveguide nonlinear kerr coefficient carrying units of $\frac{1}{Wm}$, P being the input peak power, and the dispersion length, $L_D = \frac{\tau_o^2}{|d_2|}$, τ_o is the intensity e^{-1} half duration of the pulse entering a segment, d_2 is the group velocity dispersion coefficient [19].

The relative magnitude of these characteristic lengths to each other dictate what regime of supercontinuum generation the pulse is undergoing at a segment in the alternating dispersion structure. For $R \equiv \frac{L_{nl}}{L_D} < 1$, the regime is dominated by nonlinear generation through self-phase modulation (SPM), while for $R > 1$ the regime is dispersion dominated.

In the SPM dominated regime, the spectral bandwidth enhancement due to nonlinear generation occurs primarily within the nonlinear length of the segment. Past this length, the added bandwidth accelerates the dispersive spreading of the pulse, such that final spectral saturation takes place in a distance less than the original dispersion length of the pulse entering the segment.

The dispersion dominated regime is when the additional bandwidth increase from the nonlinear generation is much less than the original bandwidth. Here, the pulse temporally spreads in approximately the same way as the original pulse would spread. The dispersion dominated regime sees much less spectral generation than the SPM dominated regime.

Moreover, R decreases for higher segment numbers in the waveguide, due to the additional frequency generation across prior segments [17], yielding shorter transform limited pulse durations. Thus, at the end of the waveguide, the region would have likely transitioned to the dispersion dominated regime, even if it was SPM dominated at the start of the waveguide

structure. In sum, the decreasing R ratio has the effect of uniformly decreasing both the saturation length and the amount of spectral broadening. For a fixed ND segment length, this translates to a decreasing AD segment length, however, we show that this length converges to a fixed constant length above zero. We show this by obtaining an expression for the AD segment lengths in the heavily dispersion dominated regime ($R \gg 1$).

In the dispersion dominated limiting case, simple expressions can be obtained, since the spectral frequency bandwidth increase at the e^{-1} per segment is then given by[17]:

$$\delta\nu \approx \left[g_o \gamma \frac{E}{4|\beta_2|} \right] , \quad (1)$$

with $g_o \approx 0.81$ being a constant related to the Gaussian pulse shape, and with E being the pulse energy.

The corresponding saturation length in the ND segment for this regime would be $L_{sat} = 2L_D$. From this the AD segment length equates to, $L_{AD} \approx (L_{ND} - L_{sat}) \left(\frac{d_{2,ND}}{d_{2,AD}} \right) + 2L_{D,AD} (1 - \delta\nu\tau_o)$. Since $\delta\nu$ stays constant while the initial pulse duration entering the ND segment decreases as segment number increases, the AD segment length converges to $L_{AD} = (L_{ND}) \left(\frac{d_{2,ND}}{d_{2,AD}} \right)$.

This has an importance consequence: Namely, for a constant ND segment length, the AD segments converge to a constant length as well, when the dispersion dominated regime is obtained. Then, periodic waveguides can be constructed, where the spectrum will always increase by Eq. 1, provided losses are negligible.

The dynamics within this regime provides another option for the sign-alternating segmented dispersion waveguides: Instead of maximal spectral increase within a few segments, where segment lengths become complicated, one can use a simple periodic arrangement of highly dispersive segments to achieve the same spectral frequency bandwidth, albeit with many more segments.

When the supercontinuum generation is SPM dominated, or in a transition region in between, ($R \approx 1$) full numerical simulation would have to be carried out to obtain AD segment lengths.

3. Effects of Uncompensated Spectral Phase and Losses

Eventually, losses and uncompensated spectral phase terminate the enhanced spectral generation of the sign-alternating dispersion waveguide structures.

The effect of losses is easily seen in the dispersion dominated regime, where a constant loss factor, $\alpha \leq 1$, between ND segments in the chain would result in a total spectral frequency bandwidth increase of: $\left(\frac{1-\alpha^n}{1-\alpha} \right) \delta\nu$, where n is the number of ND segments of the segmented waveguide. The total spectral frequency bandwidth increase then converges to a constant, $\left(\frac{1}{1-\alpha} \right) \delta\nu$, for large segment numbers instead of a linearly increasing function of segment number in the case where no losses are present.

Within the SPM and dispersion dominated regime, uncompensated spectral phase, ultimately lowers the same parameter as losses, of which nonlinear generation depends on in the ND segment: Namely, the peak intensity of the pulse entering the ND segment. However, it goes further by also increasing the pulse duration which in addition limits the total nonlinear spectral generation in the segment by effectively lowering the interaction length.

4. Convergence to Near Parabolic Spectral Phase in the SPM Dominated Regime

This section will address how higher order spectral phase can be minimized and how SCG in sign-alternating dispersion can be insensitive to higher order dispersion in such structures. Analysis will be done in the SPM dominated region of SCG in segments to highlight how SPM can modify the spectral phase profile of SCG in sign-alternating structures. Specifically shown in this section is how a near parabolic phase profile of the SCG pulse develops regardless of higher order dispersion by the influence of strong bandwidth generation by SPM.

To begin, a general condition on what segment type generates SCG with reduced higher order spectral phase must be found. For optimal pulse compression, the segments that generate spectral bandwidth are the ND segments, with nonzero GVD coefficient across the targeted bandwidth range. While, nonzero dispersion has a saturating effect on bandwidth generation, as opposed to zero dispersion systems, the spectral amplitude profile contains less modulations and the spectral phase profile does not have significant additional higher order contributions due to SPM. This can be explained by the optical wavebreaking effect [19]. Here, dispersion changes the SPM induced temporal phase function in the wings of a Gaussian-like pulse such that the phase function increases instead of saturates, i.e., its inflection is reduced. Given these spectral attributes, from here-on, only ND segments are considered to generate spectral bandwidth, where only negligible spectral generation happens in the AD segments.

Given that dispersion in ND SCG reduces the higher order spectral phase originating from SPM, it is then warranted to address how SPM in turn changes the shape of the phase function under higher order dispersion. To demonstrate how SPM influences the phase function, we perform a numerical study by solving the generalized 1-D nonlinear Schrödinger equation with dispersion terms up to the 20th order [1].

In this numerical model, we input the ND segment GVD profile of a normal dispersion fiber (Corning Hi1060flex [17]) with substantial third order dispersion (T.O.D). The GVD of this fiber is shown in Fig. 2, plotted along the envelope angular frequency range of interest. The carrier angular frequency in this example corresponds to a wavelength of 1.55 μm .

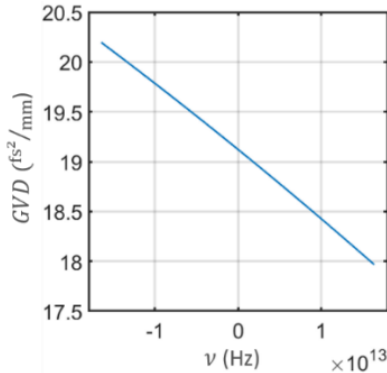


Fig. 2: Group velocity dispersion in fs^2/mm plotted with respect to envelope frequencies, across the bandwidth range of interest in an example normal dispersion fiber. This commercially available fiber, named hi1060flex, was used in [16] to build up the repeated sign-alternating SCG waveguide.

A transform limited Gaussian pulse (intensity e^{-1} of 72 fs), with a pulse energy of 2 nJ is inputted into this fiber. The peak power of this input pulse renders that SCG here is in the SPM dominated regime of the ND fiber. With these parameters, the fiber and input pulse, the characteristic spectral phase evolution of the SCG pulse can be demonstrated.

The e^{-1} angular frequency bandwidth of the spectral energy density, $\Delta\nu$, against the propagation distance, Δz , within the ND fiber is plotted in Fig. 3. The resulting saturation curve is characteristic of spectral bandwidth development in ND SCG within the SPM dominated regime. The propagation is shown up to 30 cm; the saturation length of the bandwidth development.

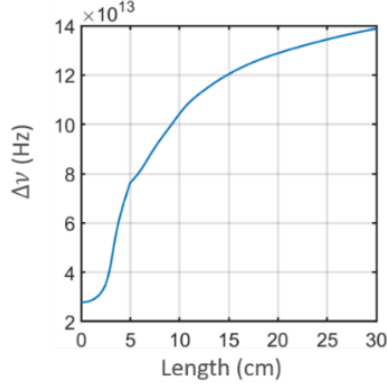


Fig. 3: The e^{-1} angular frequency bandwidth of the spectral energy density (in Hz) versus propagation distance up to the saturation length in the normal dispersion fiber.

The bandwidth development directly impacts the spectral phase profile, φ . This can be seen in how the relative magnitudes of Taylor coefficients of the spectral phase function, taken about the central angular frequency, ν_o , changes along the propagation coordinate.

We start by discussing the dependence of the of the 2nd order spectral phase coefficient, $\beta_2 \equiv \left. \frac{d^2\varphi}{d\nu^2} \right|_{\nu_o}$ on bandwidth development along the propagation of the fiber. Before spectral stagnation occurs, the pulse e^{-1} intensity duration, τ_o , and spectral bandwidth, $\Delta\nu$, increases. The increase in bandwidth decreases the transform limited duration of the pulse, $\tau_{lim} \propto \frac{1}{\Delta\nu}$. This subsequently increases the ratio of $\frac{\tau_o}{\tau_{lim}}$. Thus, more spectral phase would have to be added across the spectral profile to stretch the temporal duration of the pulse from τ_{lim} to τ_o and this fact then causes an increase of β_2 . However, due to the asymptotic nature of τ_{lim} on bandwidth, past a certain propagation distance, the ratio of $\frac{\tau_o}{\tau_{lim}}$ saturates this then correspondingly stops increasing β_2 . While, the ratio of $\frac{\tau_o}{\tau_{lim}}$ directly impacts β_2 , so does the frequency bandwidth that is generated. Increasing the bandwidth renders that the time delay generated over the bandwidth range is larger. Therefore, β_2 which is the time delay per bandwidth must reduce if the ratio $\frac{\tau_o}{\tau_{lim}}$ stays constant.

Therefore, past a certain bandwidth value, the asymptotically decreasing τ_{lim} due to the bandwidth increase, does not counter the lowering of β_2 needed (which has to scale inversely with $1/\Delta\nu$) to counter the increased temporal stretching of the pulse due to the increased bandwidth.

In fact, the following conditions can be derived from the relationship between second order spectral phase, spectral bandwidth and the corresponding Gaussian pulse duration. β_2 reaches its peak when $\tau_o = \sqrt{2}/\Delta\nu$, is achieved at a certain propagation distance within the ND waveguide. After which $\tau_o > \sqrt{2}/\Delta\nu$ and β_2 will always be decreasing if the bandwidth remains increasing due to SPM. When this equality is satisfied, then

$$\beta_2(\Delta z) \propto \frac{\tau_o(\Delta z)}{\Delta v(\Delta z)}, \quad (2)$$

As a function of propagation in the waveguide. If τ_o is slowly increasing relative to Δv , across the fiber length, i.e., in the SPM dominated regime of ND SCG, β_2 asymptotically decreases to zero.

In a practically relevant analysis of β_2 , it is warranted to compare its development, with SPM and dispersion across the fiber, to the second order spectral phase coefficient of the pulse propagating in the waveguide under only the presence of waveguide dispersion without nonlinear effects, labelled as β_{2o} . β_{2o} is then equal to $d_2\Delta z$, d_2 is the waveguide group velocity dispersion coefficient (taken about v_o).

The ratio of second order phase coefficient with SPM to the case without versus propagation is given in Fig. 4. Here we see qualitatively the expected trend as described above, i.e., an increase in β_2 to a peak value, and then its subsequent decrease past a certain bandwidth value. Finally, when spectral development ceases, past the saturation length, the reductive effect of SPM on β_2 stops and β_2 asymptotically approaches β_{2o} i.e., the ratio plotted in Fig. 4 approaches one. While, for most of its development, β_2 , is higher than β_{2o} , and only dips to 96% the value of β_{2o} , this can be changed by increasing the saturation length of spectral development but at the expense of bandwidth generation or by using long fiber segments with small saturation lengths. It can be shown that any reductive effect of SPM on β_2 , compared to β_{2o} scales weakly with input peak power.

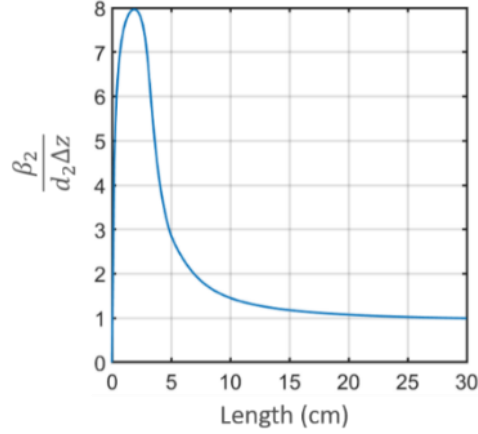


Fig. 4: Plot of the ratio of the second order spectral phase coefficient, β_2 , of the SCG pulse to that when there is no nonlinear effect, $(d_2\Delta z)$, versus propagation in the normal dispersion fiber.

In fact, this weak reduction of β_2 , is in part needed to obtain near parabolic spectral phase for ND SCG, insensitive to higher order dispersion. The other part is to show that SPM's reductive effect on the 3rd order spectral phase coefficient, β_3 is much higher. If this condition is met, the 3rd order spectral phase coefficient reduces more rapidly than the 2nd order coefficient; SPM then renders a near parabolic phase profile of the SCG pulse despite higher order dispersion as it propagates within the bandwidth saturation length of the fiber.

The β_3 coefficient follows the same trend as the β_2 coefficient, where it also is increased with $\frac{\tau_{o3}}{\tau_{lim}}$. Here, τ_{o3} is the temporal duration addition due to third order spectral phase additions (for the second order case the standard approximation $\tau_{o2} \approx \tau_o$ was used in Eq. 2 and its derivation). However, the frequency bandwidth steeper temporal stretching (time delay per

bandwidth) for third order additive phase than for second order, i.e., $\beta_3 \propto \frac{1}{\Delta\nu^2}$ instead of $\propto \frac{1}{\Delta\nu}$ as with β_2 . Therefore,

$$\beta_3(\Delta z) \propto \frac{\tau_{o3}(\Delta z)}{\Delta\nu(\Delta z)^2}, \quad (3)$$

From Eq. 3, using the assumption that $\frac{\tau_{o3}(\Delta z)}{\tau_o(\Delta z)}$ remains slowly varying compared to the bandwidth increase, $\frac{\beta_3(\Delta z)}{\beta_2(\Delta z)} \propto \frac{1}{\Delta\nu(\Delta z)}$. Therefore, it can directly be seen from Eq. 3 that as the spectral generation occurs, the spectral profile converges to parabolic in the SPM dominated regime.

Due to the higher dependence of β_3 on the bandwidth, it is expected that the maximum of β_3 will occur at a shorter propagation distance, as less bandwidth is required to overcome $\frac{\tau_{o3}}{\tau_{lim}}$. As well, the reduction of $\beta_3(\Delta z)$ would be stronger than that of $\beta_2(\Delta z)$ and will be more sensitive to bandwidth changes. Also, the peak will be smaller since the ratio of $\frac{\tau_{o3}}{\tau_{lim}}$ will be substantially smaller than $\frac{\tau_o}{\tau_{lim}}$ (τ_{lim} is larger due to reduced bandwidth where peak of β_3 occurs and τ_{o3} is smaller than τ_o due to the reduced propagation distance). This is verified in (Fig. 5) where the ratio of β_3 , to $\beta_{3o} = d_3\Delta z$ is plotted along the fiber length. β_{3o} , the 3rd order spectral phase coefficient without the influence of SPM is given by $d_3\Delta z$, d_3 is the waveguide TOD coefficient.

Fig. 5 shows that this ratio grows at first, to about 90 percent and then descends to a minimum of 13% at about 20% L_{sat} . In the region where bandwidth saturations starts to take place, the ratio then grows again and eventually approaches 1 slowly, in the asymptotical limit, for the same reasons given for the second order coefficient case (Fig. 4). However, even at the saturation length, the ratio is still only 74%.

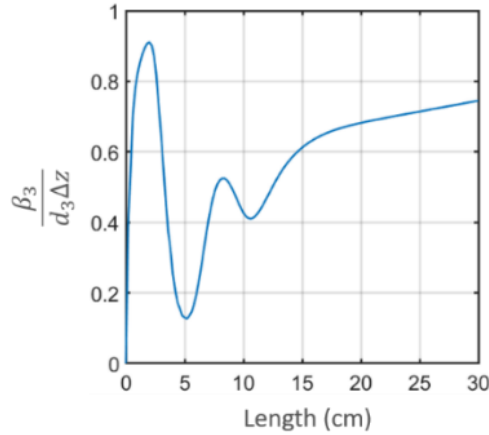


Fig. 5: Plot of the ratio of the third order spectral phase coefficient, β_3 , of the SCG pulse to the third order spectral phase coefficient in the absence of any nonlinear effect ($d_3\Delta z$) versus the propagation in the normal dispersion fiber.

It is finally verified in Fig. 6 that the normalized ratio of the two coefficients, $\left| \frac{1}{\tau_o} \frac{\beta_3}{\beta_2} \right|$ reduces along the propagation of the waveguide. It is shown in Fig. 6 that the spectral phase becomes

near parabolic regardless of higher order dispersion with the presence of SPM, as expected from the above analysis.

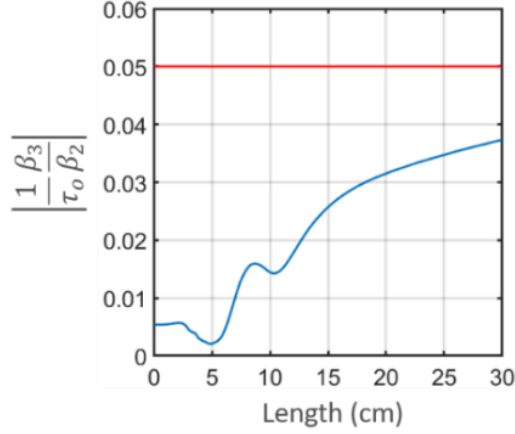


Fig. 6: Plot of the normalized ratio, $\left| \frac{1}{\tau_0} \frac{\beta_3}{\beta_2} \right|$ indicating the relative magnitude of third order dispersion coefficient to second order dispersion coefficient.

The ratio with SPM contributions stays well below the same ratio where no SPM is present (i.e., $\left| \frac{1}{\tau_0} \frac{d_3}{d_2} \right|$). In fact, this ratio dips to more than a factor of a hundred less than the linear case (0.2%), indicating a strong convergence to a parabolic profile at 20% the spectral saturation length. Moreover, the ratio stays below the linear case up to the saturation length. Since, $\frac{\beta_3}{\beta_2} = \frac{d_3}{d_2}$ for the ideal GVD of the AD segment, the substantial lowering of this ratio due to SPM, means that the AD profile GVD must be flat in the SPM dominated regime.

The above results indicate that at 20% the saturation length higher order spectral phase is minimized. Furthermore, the SCG bandwidth is close to a factor of three greater than input bandwidth at this segment length. So then, both factors; near parabolic spectral phase profile and substantial bandwidth development make this the ideal ND segment length for the alternating waveguide.

The reductive effect of SPM on spectral phase coefficients, which counters the impact of group delay dispersion, is even more pronounced at higher orders, since they depend inversely exponentially with the frequency bandwidth. For example, for 4th order, $\beta_4(\Delta z) \propto \frac{\tau_{04}(\Delta z)}{\Delta\nu(\Delta z)^3}$.

We conclude this section by noting that, due to the near parabolic spectral phase of SPM dominated ND SCG, the ideal AD dispersion profile would be a flat profile over the frequency range of interest, no matter the dispersion profile of the ND segments. While a flat AD GVD profile is ideal in the SPM dominated regime, this may not be a hard criterion since the waveguide consists of subsequent periods of ND-AD segments. After the pulse emerges from this (non-ideal) AD segment it would still go into a subsequent ND segment, where the nonlinear generation there may reduce the initial higher order spectral phase variation it has. For example, the experimental result of [17] showing that the maximum 3rd order phase contribution, occurring at the endpoints of the e^{-1} bandwidth of the SCG pulse, is a factor of three less than the linear case is explained by this behavior.

5. Additional Higher Order Phase Reduction Across Alternating Waveguides

We briefly describe two other phase compensation effects that come into play in the sign-alternating dispersion waveguides. The first is that, the non-flat GVD of Fig. 2, within an ND segment, results in an asymmetric temporal intensity profile. This works to stretch the bandwidth asymmetrically but still reduces the spectral third order phase coefficient since the endpoints of the third order spectral phase profile still are moved to frequencies away from the carrier frequency. The asymmetrical pulse profile also slows spectral generation on the blue side of frequencies, and enhanced generation on the red side thus introducing differing saturation lengths for these frequency ranges. Then, the blue end of the spectral bandwidth is generated at a larger propagation distance in the ND segment compared to the red end. The resultant increase in effective propagation distance for red frequencies and the corresponding decrease for blue frequencies results in a balancing of spectral phase that also reduces higher order contributions. In fact, the sign of β_3 could be reversed due to this phase balancing. This effect also contributes to the near-parabolic spectral phase output of the ND segments regardless of the GVD profile. The sign-reversal may open more possibilities for AD segment choices, that do not need to have opposite sign TOD to the ND segment.

The second is that in the SPM dominated regime of the alternating waveguide structure, the spectral phase becomes closer to parabolic as the pulse traverses the structure compared to the case of a uniform normal dispersion waveguide for SCG. The benefit of the alternating waveguide structure is that the pulse duration inputted to subsequent ND segments decreases, enhancing the higher order spectral phase coefficient reduction. The resultant enhancement is due to the increased bandwidth inputted into subsequent ND segments due to the reduced pulse duration.

The low higher order spectral phase coefficients, unique to our alternating waveguide structure, combined with the enhanced bandwidth at low input peak powers, then makes it an effective and powerful new scheme in nonlinear pulse compression experiments. Demonstrating potential to extend sub-cycle pulse compression to low input peak powers, removing the need for high powered drive lasers.

6. Designing Practically Feasible AD GVD Profiles for General Spectral Phase Profiles

While the above guides the choice of the AD profiles, to obtain these flat profiles for an increasing frequency range across the sign-alternating structure, is rather difficult. Moreover, there is a transition region from SPM dominated to dispersion dominated for the ND segments in the repeated sign-alternating dispersion waveguide. For these middle ND segments in the chain the ideal AD profiles become unclear. For the dispersion dominated regime, again an entirely different AD segment GVD is sought. Here, the AD segment GVD profile would be a scaled reflection of the previous ND segment GVD curve about the frequency axis, with the scaling factor determining the AD segment's length. I.e., $\text{AD GVD}(\nu) = -\epsilon \text{ND GVD}(\nu)$, $\epsilon > 0$ and the AD segment length is the previous ND segment length divided by ϵ .

Even in the SPM dominated regime, due to practical considerations, ND segments may have to exceed their saturation lengths. It is then needed to derive a practical and general method for obtaining both an overall flat AD GVD or any other needed AD GVD such that the pulse obtains a transform limited duration at the end of the segment

We proceed by splitting the AD segment into a number of sub-segments, for the goal of compensating the spectral phase of the pulse coming out of the ND segment. The overall GVD coefficient of these sub-segments is anomalous to compensate for the positive second order spectral phase coefficient of ND segment SCG. The number of such sub-segments determines the order precision of spectral phase compensation. For example, two sub-segments would

compensate up to 3rd order spectral phase, three would compensate up to 4th order and so forth. This AD segment scheme is depicted in Fig. 7.

Next, for an optical pulse having traversed these sub-segments, perfect spectral phase compensation up to order “ n ” would be achieved if the segments satisfy:

$$\begin{aligned}
 -\sum_{k=1}^n d_{2,k} L_k &= \beta_2 \equiv \left. \frac{d^2 \varphi}{dv^2} \right|_{\nu_o} \\
 -\sum_{k=1}^n d_{3,k} L_k &= \beta_3 \equiv \left. \frac{d^3 \varphi}{dv^3} \right|_{\nu_o} \\
 &\vdots \\
 -\sum_{k=1}^n d_{n,k} L_k &= \beta_n \equiv \left. \frac{d^n \varphi}{dv^n} \right|_{\nu_o}
 \end{aligned} \tag{4a}$$

Where, $d_{j,k}$ is the j^{th} dispersion coefficient (taken about ν_o) of sub-segment indexed by the number k . φ is the spectral phase of the output pulse from the ND segment entering these sub-segments. ν is the angular frequency and ν_o is the central angular frequency of the pulse, about where the Taylor series expansion of the spectral phase occurs. L_k is the length of the specific sub-segment.

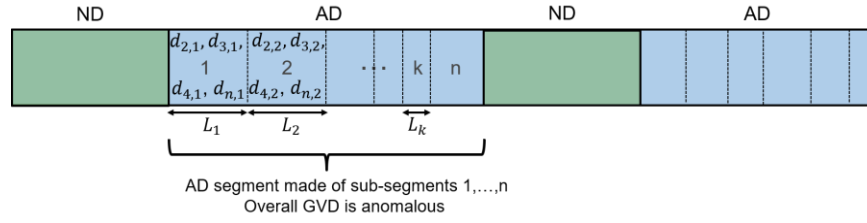


Fig. 7: AD segments can be split into subsegments where the sub-segment dispersion coefficients satisfy Eq. 4.

Equation 4a can be conveniently represented in matrix form,

$$\mathbf{Ax} = \mathbf{y} \tag{4b}$$

Where, \mathbf{A} is a $n - 1$ by k matrix formed with the d 's as elements, i.e., $d_{j,k}$ (rows labelled by index j , columns by index k). \mathbf{x} is a column vector of segment lengths, and \mathbf{y} is a column vector of increasing derivative orders, starting from 2nd to n^{th} order of the spectral phase of the pulse exiting the ND segment at ω_o .

In general, $d_{j,k}$ need not be the same sign, however, materials must be chosen such that at the end all L_k that solve this system of equations must be positive, so that the solution is physically relevant. Also, the waveguide sub-segments must be chosen such that n linearly independent equations are guaranteed. This is easy to guarantee if there is variation in the segment geometry or materials.

in a practical setting the number of sub-segments is strongly limited by coupling losses in-between these sub-segments. This puts strict criteria on the mode field diameters (MFD) of these waveguide segments. Thus, the sub-segments must vary their geometry (e.g., core diameter) in an adiabatic way, or in a perturbative sense in relation to neighboring sub-segments.

This would introduce small variations in the segment dispersion coefficients in relationship to one another so that longer segment lengths are present in the sign-alternating dispersion waveguide. In general, this is only a problem if propagation losses are substantial, especially compared to coupling losses that would be introduced if the adiabatic variation between sub-segments is broken.

7. Summary

We explored the conditions that lead to the AD and ND segment lengths of repeated sign-alternating dispersion SCG waveguides to converge to a constant for both segment types. This has ramifications both in the practical design of these structures and whether they can be used in resonator configurations.

Next, we explored the spectral phase development of the SCG where we find a previously unknown phase effect in supercontinuum generation within normal dispersion waveguides. Namely, that the spectral phase demonstrates robustness to higher order dispersion. This result is amplified within our sign-alternating structures, rendering that our waveguide concept combines a near parabolic spectral phase profile with a substantially increased bandwidth generation. Thus, we foresee that our scheme has potential for sub-cycle pulse compression without the onus of high peak power drive lasers. This then provides an efficient scheme for nonlinear pulse compression for a greater plethora of optical platforms such as for high repetition rate lasers and integrated photonic applications.

We then outlined a practical design method to obtain ideal AD segment GVD profiles needed to compensate all spectral phase terms coming from the corresponding ND segments. These results are not only applicable to repeated sign-alternating SCG waveguides but for general nonlinear pulse compression schemes.

Funding

The authors would like to acknowledge funding from the MESA+ Institute of Nanotechnology within the grant “Ultrafast switching of higher-dimensional information in silicon nanostructures”.

Acknowledgments

The authors would like to thank Klaus-Jochen Boller for useful discussions and input. Portions of this work will be presented at the High-brightness Sources and Light-driven Interactions Congress in 2020.

Disclosures

The author is a co-inventor for a pending filed patent owned by University of Twente of which a part is related to this work. The patent application no. is 16/204,614.

References

1. J. M. Dudley, G. Genty, and S. Coen, "Supercontinuum generation in photonic crystal fiber," *Rev. Mod. Phys.* **78**, 1135–1184 (2006).
2. A. M. Heidt, J. S. Feehan, J. H. V. Price, and T. Feurer, "Limits of coherent supercontinuum generation in normal dispersion fibers," *J. Opt. Soc. Am. B* **34**, 764 (2017).
3. C. Manzoni, O. D. Mücke, G. Cirimi, S. Fang, J. Moses, S.-W. Huang, K.-H. Hong, G. Cerullo, and F. X. Kärtner, "Coherent pulse synthesis: towards sub-cycle optical waveforms." *Laser Photonics Rev.* **9**(2), 129-171(2015).

4. M.T. Hassan, T.T. Luu, A. Moulet, O. Raskazovskaya, P. Zhokhov, M. Garg, N. Karpowicz, A.M. Zheltikov, V. Pervak, F. Krausz and E. Goulielmakis, "Optical attosecond pulses and tracking the nonlinear response of bound electrons," *Nature* **530**(7588), pp.66-70(2016).
5. M. Hemmer, M. Baudisch, A. Thai, A. Couairon, and J. Biegert, "Self-compression to sub-3-cycle duration of mid-infrared optical pulses in dielectrics," *Opt. Express* **21**, 28095 (2013).
6. H.-W. Chen, H. Zia, J. K. Lim, S. Xu, Z. Yang, F.X. Kärtner, and G. Chang, "3 GHz, Yb-fiber laser-based, few-cycle ultrafast source at the Ti: sapphire laser wavelength." *Opt. Lett.* **38**, 4927-4930(2013).
7. M. Yu, Y. Okawachi, A. G. Griffith, N. Picqué, M. Lipson, and A.L. Gaeta, "Silicon-chip-based mid-infrared dual-comb spectroscopy," *Nat. Commun.*, **9**(1), 1-6 (2018).
8. K. Luke, Y. Okawachi, M. R. E. Lamont, A. L. Gaeta and M. Lipson, "Broadband mid-infrared frequency comb generation in a Si₃N₄ microresonator," *Opt. Lett.* **40**, 4823 (2015).
9. A. Schliesser, N. Picqué, and T. W. Hänsch, "Mid-infrared frequency combs," *Nat. Photonics* **6**, 440–449 (2012).
10. G. B. Rieker, F. R. Giorgetta, W. C. Swann, J. Kofler, A. M. Zolot, L. C. Sinclair, E. Baumann, C. Cromer, G. Petron, C. Sweeney, P. P. Tans, I. Coddington, and N. R. Newbury, "Frequency-comb-based remote sensing of greenhouse gases over kilometer air paths," *Optica* **1**, 290 (2014).
11. R. Holzwarth, "Optical frequency metrology" *Nat. Rev.* **416**, 1–5 (2002).
12. G. Humbert, W. J. Wadsworth, S. G. Leon-Saval, J. C. Knight, T. A. Birks, P. St. J. Russell, M. J. Lederer, D. Kopf, K. Wiesauer, E. I. Breuer, and D. Stifter. "Supercontinuum generation system for optical coherence tomography based on tapered photonic crystal fibre," *Opt. Express* **14**, 1596 (2006).
13. A. Unterhuber, B. Považay, K. Bizheva, B. Hermann, H. Sattmann, A. Stingl, T. Le, M. Seefeld, R. Menzel and M. Preusser, "Advances in broad bandwidth light sources for ultrahigh resolution optical coherence tomography," *Phys. Med. Biol.* **49**, 1235–1246 (2004).
14. N. M. Israelsen, C. R. Petersen, A. Barh, D. Jain, M. Jensen, G. Hanneschlaeger, P. Tidemand-Lichtenberg, C. Pedersen, A. Podoleanu, and O. L. Bang, "Real-time high-resolution mid-infrared optical coherence tomography," *Light Sci. Appl.* **8**, (2019).
15. Q. Du, Z. Luo, H. Zhong, Y. Zhang, Y. Huang, T. Du, W. Zhang, T. Gu, and J. Hu, "Chip-scale broadband spectroscopic chemical sensing using an integrated supercontinuum source in a chalcogenide glass waveguide," *Photon. Res.* **6**, 506-510 (2018).
16. C.F. Kaminski, R.S. Watt, A.D. Elder, J.H. Frank, and J. Hult, "Supercontinuum radiation for applications in chemical sensing and microscopy," *Appl. Phys. B* **92**, 367 (2008).
17. H. Zia, N. M. Lüpken, T. Hellwig, C. Fallnich, and K. J. Boller, "Supercontinuum generation in media with sign-alternated dispersion," arXiv preprint arXiv:1905.01820 (2019).
18. S. Xie, F. Tani, J. C. Travers, P. Uebel, C. Caillaud, J. Troles, M. A. Schmidt, and P. St. J. Russel, "As₂S₃-silica double-nanospike waveguide for mid-infrared supercontinuum generation," *Opt. Lett.* **39**, 5216-5219(2014).
19. Alfano, R. R. *The supercontinuum laser source: the ultimate white light.* (Springer US, 2016).
20. A. M. Heidt, J. Rothhardt, A. Hartung, H. Bartelt, E. G. Rohwer, J. Limpert, and A. Tünnermann, "High quality sub-two cycle pulses from compression of supercontinuum generated in all-normal dispersion photonic crystal fiber," *Opt. Express* **19**, 13873 (2011).

21. S. Demmler, J. Rothhardt, A. M. Heidt, A. Hartung, E. G. Rohwer, H. Bartelt, J. Limpert, and A. Tünnermann, "Generation of high quality, 1.3 cycle pulses by active phase control of an octave spanning supercontinuum, " *Opt. Express* **19**, 20151(2011).
22. I. A. Sukhoivanov, S. O. Iakushev, O. V. Shulika, J. A. Andrade-Lucio, A. Díez, and M. Andrés, "Supercontinuum generation at 800 nm in all-normal dispersion photonic crystal fiber, " *Opt. Express* **22**, 30234 (2014).
23. S. Xing, S. Kharitonov, J. Hu, and C. S. Brès, "Linearly chirped mid-infrared supercontinuum in all-normal-dispersion chalcogenide photonic crystal fibers, " *Opt. Express* **26**, 19627 (2018).